Analysis and Optimization of Continuous Organic Solvent Nanofiltration by Membrane Cascade for Pharmaceutical Separation

Ricardo Abejón, Aurora Garea, and Angel Irabien
Departamento de Ingenierías Química y Biomolecular, Universidad de Cantabria, Avda. Los Castros s/n, 39005 Santander, Cantabria, Spain

DOI 10.1002/aic.14345
Published online January 13, 2014 in Wiley Online Library (wileyonlinelibrary.com)

The major part of the production costs of pharmaceuticals can be imputed to the downstream processing, where membrane technologies have to deal with some challenges as separations involving solutes with similar sizes or solvent recovery and recycling. This work contributes to the progress in the design of continuous organic solvent nanofiltration systems for this purpose and includes the configuration of dual membrane cascades, sensitivity analysis of the operation variables, and economic optimization as innovations. Analyzed configurations include multistage cascades up to three stages, and dual membrane cascades up to five stages. The total costs (TC) were chosen as the formulated objective function to minimize in the economic optimization strategy. The treatment of the residual stream leaving the system resulted the main cost of the process (more than 85% for dual cascades), but the solvent recovery units can significantly reduce the TC (64–77% depending on the required solvent quality). © 2014 American Institute of Chemical Engineers *AIChE J*, 60: 931–948, 2014

Keywords: membrane cascade, organic solvent nanofiltration, pharmaceuticals, sensitivity analysis, multiobjective optimization

Introduction

Downstream processing is a critical part of the biotechnological and pharmaceutical production processes. For nearly all the products manufactured by these two industrial sectors, one starts with a dilute suspension and tries to produce a highly purified dry product. Most of the downstream processes include these four main steps: removal of insoluble particles, isolation of the product, purification, and polishing.[1] The major part of the production costs of pharmaceuticals can be imputed to the downstream processing: the low effectiveness of the downstreaming steps of a bioprocess causes that it should be considered as the most expensive part of the whole process, as the recovery costs normally exceed the costs of the rest of the bioprocess.[2] The adequate solute separation, concentration, and sometimes fractionation is, therefore, crucial to secure a pure final product while avoiding excessive costs.

Several techniques are available for the treatment of the solutes, including distillation, crystallization, chromatography, adsorption–desorption, ion exchange, extraction, molecular imprinting, and membranes.[3,4] Most membrane technologies have found room in downstream processing: microfiltration,[5] ultrafiltration,[6] nanofiltration,[7] and reverse osmosis.[8] Focusing on nanofiltration, this technique can separate solutes based on their molecular weights and sizes. Organic solvent resistant membranes have been developed for the last years and they are nowadays applied to multiple tasks in the downstreaming framework.[9–14]

Some of these nanofiltration examples use diafiltration. However, diafiltration has many limitations, as it can be found in bibliography.[15] Among them, the difficulties to operate in continuous mode (it is more oriented to batchwise processes) have to be remarked. Continuous processing has been identified as one of the most important key research areas for making advances in green engineering in the pharmaceuticals and fine chemicals productive fields. Therefore, it should be prioritized.[16] Continuous processing is seen as a very adequate option to improve the sustainability of the corresponding operations, but it is not yet generally applied wherever advantageous.[17] When applied to pharmaceutical manufacturing, the justification of continuous processing includes many advantages in several aspects such as economy, product quality, environmental impact, and safety.

The solute separation processes by nanofiltration can achieve high product purity and process yield when the solutes to be separated show appreciable differences in their molecular sizes. The more challenging separations involving solutes with closer sizes cannot be carried out by single-stage processes, so additional stages become necessary. Membrane cascades have demonstrated their potential as a satisfactory configuration that includes several stages to overcome the constraints of limited separation processes. The design of membrane cascades has been deeply

Correspondence concerning this article should be addressed to A. Garea at gareaa@unican.es.

studied,[18–20] and the most important types of membranes according to pore diameter have been used under a cascade scheme, from microfiltration[21] to reverse osmosis.[22] Ultrafiltration and nanofiltration are the most frequently used membrane technologies for biotechnological and pharmaceutical purposes. Ultrafiltration is widely used for the separation and fractionation of proteins and other biological molecules[23–32] and nanofiltration cascades have been implemented for pesticide removal,[33] solvent exchange,[34] solvent recovery,[35] and separation and fractionation of pharmaceutical solutes.[3,15,36]

Despite the number of references in which the use of membrane cascade is described, the analysis of the performance of such a system in continuous mode as a function of operational variables and cascade design is missing. Without these data, the design of optimal cascades is impossible. While significant progress has been achieved in the last years in the design of downstream processing, there is work to be done to apply the full potential of the tools provided by process systems engineering.[37,38] Although the pharmaceutical industry has been traditionally reluctant to introduce innovative methods in its production processes, some recent experiences show the benefits of taking into consideration these useful tools.[39,40] Some efforts have been specifically pointed to the downstream process development,[41,42] and the optimization of membrane processes has been investigated in this field.[43,44]

This article contributes to the progress in the design of continuous downstream processing systems that take advantage of the employment of membrane cascades. The performance of cascades when applied to pharmaceutical separations has been scarcely investigated. Hence, tools provided by process systems engineering were applied in a novel approach to carry out a complete analysis of this type of processes. The work includes a sensitivity analysis of the main operation variables and an economic evaluation, prior to the optimization of the system configuration and the determination of the optimal values for the corresponding process variables to minimize the costs of the process.

As a case study, the separation of an intermediate precursor of an anesthetic compound from an impurity was selected. Fentanyl is extensively used for anesthesia and analgesia in operating rooms and intensive care units as it is a synthetic opioid 50–100 times more potent than morphine.[45] Fentanyl is characterized by a rapid onset of analgesia and a relatively short duration of action, but the emphasis in anesthetic and surgical practice focusing on shorter and outpatient surgical procedures requires the use of ultrashort acting opioids.[46] Alfentanil is a fentanyl-analogous substance with around a quarter the potency of fentanyl and around a third of the duration of action, but with an onset of effects four times faster than fentanyl.[47] The 1-(2-bromoethyl)-4-ethyl-1,4-dihydro-5H-tetrazol-5-one (Compound A) is needed as intermediate in the preparation of alfentanil but during the synthesis process it has to be separated from an impurity, ethylene bromide (Compound I), in a very challenging separation due to the similar size of both solutes ($MW_A = 221$ g/mol and $MW_I = 188$ g/mol).

Continuous Process Modeling

Multiple configurations of organic solvent nanofiltration membrane cascades can be considered, and the final establishment of each design would depend on the specific separation targets. Detailed analysis of the main types of cascades

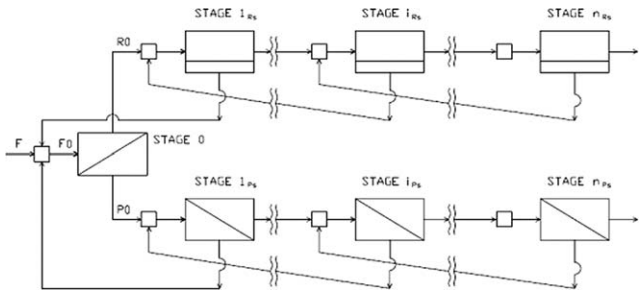

Figure 1. General scheme of a dual membrane cascade.

can be found in bibliography.[15,36] In this article, the dual membrane cascade was selected to perform the proposed separation process. Figure 1 shows a general scheme of a dual membrane cascade comprising multistage retentate section (retentate streams integrated in series to purify the least permeable solute) and multipass permeate section (permeate streams integrated in series to purify the most permeable solute), which could be considered, respectively, equivalent to the stripping and purifying sections defined by other authors when the solute fractionation cascades are described.[3] This way, the dual cascade appears as a more effective system for solute separation and fractionation than conventional cascades fed on one end. The use of the "stripping" and "purifying" terms makes reference to the classical denomination of the sections of a distillation column, while "multistage" and "multipass" expressions are much more usual in the membrane separation field.

A stage is defined as a membrane unit fed with retentate from a previous membrane unit when talking about membrane networks. The use of multistage systems is quite common in seawater desalination plants as it is useful to obtain more fresh water from retentate streams.[48] This configuration appears to be very desirable for the case of brackish water desalination, as the concentrate from a first stage would maintain a sufficiently low salinity and could be easily desalinated in a second-stage unit.[49]

A pass is defined as a membrane unit fed with permeate from a previous membrane unit. Multipass arrangement is an effective way of achieving exigent permeate quality requirements when poor retention is such that the membrane is unavailable to reach the desired rejection in a single stage. This configuration offers an appropriate solution to the poor rejection of the boron found in seawater, so some desalination plants are configured in this way.[50,51] It can also be applied to some industrial sectors that require specific high-quality permeates as in the case of ultrapure chemicals.[52]

As it can be seen in Figure 1, the feed stream F enters the system through the Stage 0. The separation process performed by the membrane produces two output streams: the retentate stream $R0$, which would feed the initial stage of the multistage retentate section of the cascade (Stage 1_{Rs}) and the permeate stream $P0$, which would feed the initial stage of the multipass permeate section of the cascade (Stage 1_{Ps}). The main objectives of the retentate section are to purify the most retained solute and to avoid the loss of the most permeable solute. On the contrary, the permeate section performs an increase in the purity of the most permeable solute, while reduces the amount of the most retained solute that can leave the system by this way. The recirculation of the permeate streams in the retentate section and the retentate streams of the permeate section to the corresponding previous stages

configures a countercurrent cascade that improves the efficiency of the system. In this case, there is a unique stream entering the cascade (feed stream F) as it was decided to avoid the use of any auxiliary pure solvent stream that can be added to the cascade according to different criteria (improvement of the separation performance, control of solute precipitation, or minimization of solubility problems).

A complete simulation model based on equations for solvent and solute transport through membranes and mass balances (overall and by components) was formulated to represent the dual membrane system (membrane modules and mixers). The economic evaluation was performed by a simple economic model proposed to estimate the main costs of the process.

Membrane transport

Several alternatives are proposed to obtain transport equations for the nanofiltration membranes: the solution-diffusion model,[53] the solution-diffusion with imperfections,[54] the Kedem–Katchalsky model,[55] or the Spiegler–Kedem model.[56] According to the previous experience of this research group taken after testing different models to represent the performance of low-pressure reverse osmosis membranes,[57] the Kedem–Katchalsky model can be considered as an attractive option to simulate the transport through nanofiltration membranes. Specific organic solvent nanofiltration models will be tested in further work.[58–60]

The Kedem–Katchalsky model,[61] simplified by consideration of negligible osmotic pressure contributions by diluted solutions, defines the characteristic variables of the nanofiltration membrane behavior, the specific permeate flux (J_V), and the retention coefficient of each solute (R^{sol}) as functions of the applied pressure

$$J_V = L_P \Delta P \tag{1}$$

$$R^{sol} = \sigma^{sol} \frac{J_V}{J_V + \omega^{sol}} \tag{2}$$

where ΔP is the applied pressure and L_P, σ^{sol}, and ω^{sol} are the Kedem–Katchalsky parameters: hydraulic permeability coefficient, solute reflection coefficients, and modified solute permeability coefficients, respectively.

Mass balances

Once the membrane transport was defined, the characteristics of the permeate streams (flow P and solute concentrations cP^{sol}) could be calculated as function of the membrane area of the corresponding stage

$$P = A \cdot J_V \tag{3}$$

$$cP^{sol} = cF^{sol}\,(1 - R^{sol}) \tag{4}$$

The overall and component (solute) mass balances applied to each stage were composed for both membrane modules and mixers:

Feed stage module

$$F0 = P0 + R0 \tag{5}$$

$$F0 \cdot cF0^{sol} = P0 \cdot cP0^{sol} + R0 \cdot cR0^{sol} \tag{6}$$

Retentate side modules

$$F(i)_{Rs} = P(i)_{Rs} + R(i)_{Rs} \tag{7}$$

$$F(i)_{Rs} \cdot cF(i)^{sol}_{Rs} = P(i)_{Rs} \cdot cP(i)^{sol}_{Rs} + R(i)_{Rs} \cdot cR(i)^{sol}_{Rs} \tag{8}$$

Permeate side modules

$$F(i)_{Ps} = P(i)_{Ps} + R(i)_{Ps} \tag{9}$$

$$F(i)_{Ps} \cdot cF(i)^{sol}_{Ps} = P(i)_{Ps} \cdot cP(i)^{sol}_{Ps} + R(i)_{Ps}\, cR(i)^{sol}_{Ps} \tag{10}$$

Feed stage mixer

$$F + P(1)_{Rs} + R(1)_{Ps} = F0 \tag{11}$$

$$F \cdot cF^{sol} + P(1)_{Rs} \cdot cP(1)^{sol}_{Rs} + R(1)_{Ps} \cdot cR(1)^{sol}_{Ps} = F0 \cdot cF0^{sol} \tag{12}$$

Retentate side mixers

$$R(i-1)_{Rs} + P(i+1)_{Rs} = F(i)_{Rs} \tag{13}$$

$$R(i-1)_{Rs} \cdot cR(i-1)^{sol}_{Rs} + P(i+1)_{Rs} \cdot cP(i+1)^{sol}_{Rs} = F(i)_{Rs} \cdot cF(i)^{sol}_{Rs} \tag{14}$$

Permeate side mixers

$$P(i-1)_{Ps} + R(i+1)_{Ps} = F(i)_{Ps} \tag{15}$$

$$P(i-1)_{Ps} \cdot cP(i-1)^{sol}_{Ps} + R(i+1)_{Ps} \cdot cR(i+1)^{sol}_{Ps} = F(i)_{Ps} \cdot cF(i)^{sol}_{Ps} \tag{16}$$

Last mixer of the retentate side

$$R(n-1)_{Rs} = F(n)_{Rs} \tag{17}$$

$$R(n-1)_{Rs} \cdot cR(n-1)^{sol}_{Rs} = F(n)_{Rs} \cdot cF(n)^{sol}_{Rs} \tag{18}$$

Last mixer of the permeate side stage

$$P(n-1)_{Ps} = F(n)_{Ps} \tag{19}$$

$$P(n-1)_{Ps} \cdot cP(n-1)^{sol}_{Ps} = F(n)_{Ps} \cdot cF(n)^{sol}_{Ps} \tag{20}$$

The recovery ratio of each stage (Rec(i)) can be defined as

$$\mathrm{Rec}(i) = \frac{P(i)}{F(i)} \tag{21}$$

The performance of the membrane continuous installations were evaluated by the analysis of some process parameters such as product purity, process yield, and the concentration factor (CF) of the product when compared to the raw feed. In the case of a solute of interest A, and an impurity I, these process parameters are defined as

$$\mathrm{Purity} = 100 \frac{cR(n)^{A}_{Rs}}{cR(n)^{A}_{Rs} + cR(n)^{I}_{Rs}} \tag{22}$$

$$\mathrm{Yield} = 100 \frac{R(n)_{Rs} \cdot cR(n)^{A}_{Rs}}{F \cdot cF^{A}} \tag{23}$$

$$\mathrm{CF} = \frac{cR(n)^{A}_{Rs}}{cF^{A}} \tag{24}$$

Estimation of costs

Some basic economic considerations were taken into account to formulate an economic model based on the costs of the process. The total costs (TC) of the system were calculated by the addition of the capital costs (CC) and the operation costs (OC). The CC attributable to membranes or

Table 1. Kedem–Katchalsky Model Parameters for the Case of Study

	Compound A	Compound I
σ	0.688	0.172
ω (m/d)	1.38×10^{-1}	4.65×10^{-1}
ω (m/s)	1.60×10^{-6}	5.38×10^{-6}
L_P (m/d bar)	4.69×10^{-2}	
L_P (m/s bar)	5.43×10^{-7}	

to the rest of the installation were differentiated, whereas the OC were itemized into energy, labor, maintenance, chemical losses, and waste treatment costs

$$\mathrm{TC} = \mathrm{CC} + \mathrm{OC} \tag{25}$$

$$\mathrm{CC} = \mathrm{CC}_{\mathrm{memb}} + \mathrm{CC}_{\mathrm{inst}} \tag{26}$$

$$\mathrm{OC} = \mathrm{OC}_{\mathrm{en}} + \mathrm{OC}_{\mathrm{lab}} + \mathrm{OC}_{\mathrm{m}} + \mathrm{OC}_{\mathrm{loss}} + \mathrm{OC}_{\mathrm{waste}} \tag{27}$$

The CC of the membranes modules considering straight-line depreciation were expressed as function of the total membrane area of the installation

$$\mathrm{CC}_{\mathrm{memb}} = \frac{\sum \mathrm{A}(i)}{\mathrm{LT}_{\mathrm{memb}}} Y_{\mathrm{memb}} \tag{28}$$

Once the membranes costs were defined, the CC corresponding to the rest of the installation were related to them by mean of a coefficient (K_{memb}) that expressed the contribution of the investment in membranes to the total CC. Bibliographic references[62,63] estimate the percentage of the total investment attributable to the membranes in the range 12–30% for reverse osmosis processes. However, in the case of organic solvent nanofiltration, this contribution is usually lower and a value of 2.5% that can be found in bibliography was assumed.[36]

$$\mathrm{CC}_{\mathrm{inst}} = \mathrm{CC}_{\mathrm{memb}} \frac{(1-K_{\mathrm{memb}})}{K_{\mathrm{memb}}} \frac{\mathrm{LT}_{\mathrm{memb}}}{\mathrm{LT}_{\mathrm{inst}}} \tag{29}$$

The OC are essentially based on the consumption of the corresponding resource, except for the case of maintenance costs, which were expressed as a function of the CC (in this formulation, the maintenance costs are calculated as 5% of the total CC)

$$\mathrm{OC}_{\mathrm{m}} = 0.05 \cdot \mathrm{CC} \tag{30}$$

The energy costs were attributable to the pressurization of the feed streams which enter the membrane modules. The energy source used was electricity, and the yield of the pumps is a factor that affects the total consumption

$$\mathrm{OC}_{\mathrm{en}} = \frac{\sum F(i) \cdot \Delta P(i)}{36 \cdot \eta} Y_{\mathrm{elec}} \tag{31}$$

The installation was designed to be totally operated by a single worker, who can manage the complete system without stress

$$\mathrm{OC}_{\mathrm{lab}} = 24 \cdot Y_{\mathrm{sal}} \tag{32}$$

As the total recovery of the desired Compound A is not attainable, part of it leaves the system into the waste stream, so this loss of chemical has to be accounted for in the OC. Anyway, as the lost chemical is impure and quite diluted, it has to be valued lower than the price of the pure chemical

$$\mathrm{OC}_{\mathrm{loss}} = P(n)_{\mathrm{Ps}} \cdot cP(n)^{\mathrm{A}}_{\mathrm{Ps}} \cdot Y_{\mathrm{loss}} \tag{33}$$

The stream leaving the system as permeate stream of the last module in the permeate section of the cascade should be considered as a waste stream that is enriched in the impurity compound when compared with the initial feed stream. This waste stream needs to be treated and the corresponding treatment costs were formulated

$$\mathrm{OC}_{\mathrm{waste}} = P(n)_{\mathrm{Ps}} \cdot Y_{\mathrm{waste}} \tag{34}$$

Results and Discussion

Membrane performance and transport modeling

The experimental results for the separation of the intermediate precursor Compound A from the impurity Compound I with methanol as solvent when using the Duramem 200 membrane can be found in bibliography.[36] These results were adjusted to the Kedem–Katchalsky model and the obtained parameters are shown in Table 1. The dependence of the applied pressure over the permeate flux and the solute rejection coefficients can be observed in Figure 2.

It is obvious that the Compound I is poorly rejected by the membrane as the maximum achieved rejection coefficient is lower than 0.2, whereas values close to 0.6 can be found for the Compound A. Besides, the increase in the rejection coefficient with the applied pressure is more pronounced for the Compound A, so the difference in the rejection of the solutes would increase with this operation variable (better separation should be expected at high pressure).

The Kedem–Katchalsky can be useful to have a first approach to the understanding of the transport phenomena through the membrane. The solute flux from the feed side to the permeate side of a membrane can be expressed in terms of the Kedem–Katchalsky model as follows

$$J^{\mathrm{sol}} = \omega^{\mathrm{sol}} \Delta c^{\mathrm{sol}} + J_{\mathrm{V}}(1-\sigma^{\mathrm{sol}}) c^{\mathrm{sol}}_{\mathrm{ln}} \tag{35}$$

This way, the flux of each solute across the membrane is the sum of diffusive and convective contributions: a concentration difference on both sides of the membrane causes diffusive transport, and solute transport by convection takes place because of an applied pressure gradient across the membrane.[56] The values of both contributions were calculated from the obtained model parameters to establish the relative importance of both transport mechanisms and it is shown in Table 2 as the percentage of solute flux due to diffusion for each compound.

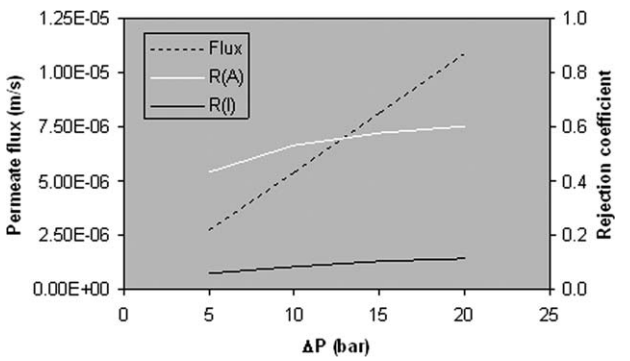

Figure 2. Permeate flux and rejections coefficients according to the Kedem–Katchalsky model.

Table 2. Percentage Contribution of the Diffusive Term to the Total Solute Fluxes

	Diffusive Contribution to Total Solute Flux (%)	
ΔP	Compound A	Compound I
5	51.7	12.4
10	41.7	9.7
15	35.0	8.0
20	30.2	6.8

At low pressures, both contributions are very similar for the transport of the Compound A, and the diffusive term is only a bit higher than the convective one. However, on applying high pressures, the second term (convective) increases to be dominant. The convective contribution is the main one for the Compound I for the entire pressure range.

Characterization and analysis of the performance of the single-stage continuous process

The characterization of the nanofiltration system in a single-stage process is an essential step for the design of a membrane cascade. To evaluate the performance of the system, four process parameters (product purity, product yield, CF, and total membrane area) were analyzed as functions of the applied pressure and the recovery rate of the stage. ASPEN Custom Modeler was used as simulation software for the evaluation, and as initial values, a feed stream of 1 m^3/h was selected, with concentrations of 25 and 75 ppm for the Compounds A and I, respectively, which corresponds to a purity of 25% as defined in Eq. 22. Such diluted concentrations were selected to avoid problems related to solute solubility or appearance of new liquid phases, and although they cannot be considered as representative of the industrial-scale process selected as case of study, the more general perspective of this article can justify these assumptions (the case of study reported has the only purpose to illustrate, without anyway limiting, the optimal use of dual cascades for advanced separation processes). Nevertheless, these initial conditions could be more related to reprocessing of auxiliary solvent streams with low solute content or downstream processing of the product streams after chemical and biological reactions in a very diluted scenario.

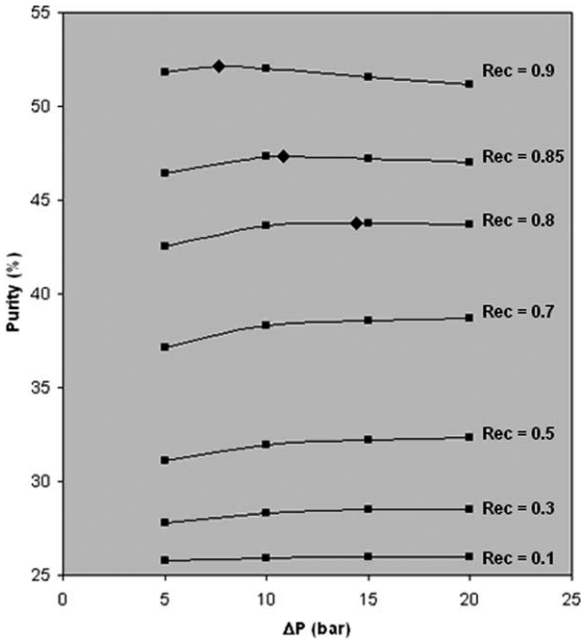

Figure 3. Evolution of the product purity as function of the applied pressure and the recovery rate for a single-stage process (diamonds indicate maximum values).

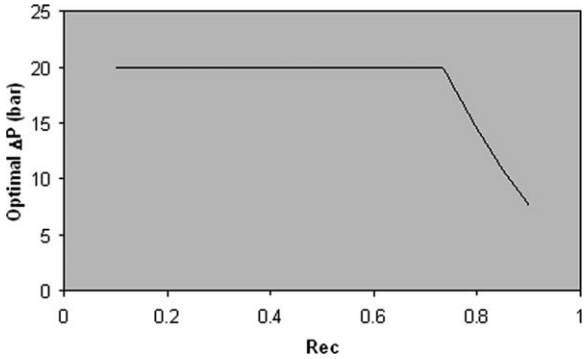

Figure 4. Optimal pressure profile to maximize the purity of the product obtained by the single-stage process.

The evolution of the product purity can be observed in Figure 3. The influence of the recovery rate over the purity is quite clear: the higher the recovery rate, the purer the obtained product. Taking into account that the feed stream has a purity of 25%, the system is able to double this value when working with a recovery rate of 0.9. The maximum value that can be reached under these conditions is 52.1% when an applied pressure of 7.6 bar is chosen. It is obvious that high recovery rates imply high permeate flows. As in this case the desired product is the least permeable one, the undesired impurity will permeate in a greater quantity when high recovery rates are chosen, and consequently, the purity of the retentate stream will increase.

The influence of the applied pressure is a bit more complex; while the optimum value is the fixed maximum limit (20 bar) for all the recovery rates lower than 0.8, the three higher recovery rates have optimum pressures different from 20 bar: 14.4, 10.8, and 7.6 bar for the 0.8, 0.85, and 0.9 recovery rates, respectively (these points are represented as diamonds in Figure 3). Further investigation was carried out to obtain the optimal pressure profile and it is shown in Figure 4. The value of 20 bar is maintained as the optimum pressure until recovery rate becomes higher than 0.73. After this point, the profile follows a decreasing curve, although very close to a straight line, to reach its minimum value (7.6 bar for 0.9 recovery rate).

A deeper look to understand this result can be taken by the study of the relationships between the process parameter and the operation variables. The purity of a single-stage system can be expressed as

$$\text{Purity} = 100\frac{cR0^{\text{A}}}{cR0^{\text{A}} + cR0^{\text{I}}} = 100\frac{cF^{\text{A}}[1-\text{Rec}(1-R^{\text{A}})]}{cF^{\text{A}}[1-\text{Rec}(1-R^{\text{A}})] + cF^{\text{I}}[1-\text{Rec}(1-R^{\text{I}})]} \quad (36)$$

To maximize the purity, the first addend in the denominator, which is the term corresponding to the least permeable compound, should be as high as possible, whereas the second addend, which corresponds to the most permeable

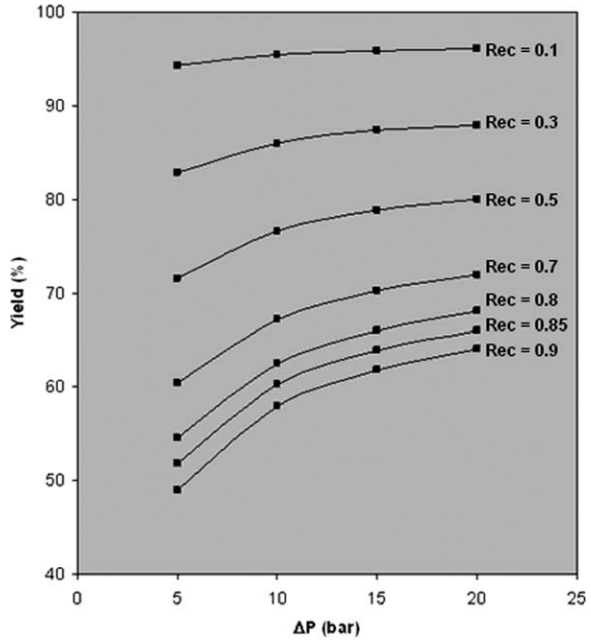

Figure 5. Evolution of the product yield as function of the applied pressure and the recovery rate for a single-stage process.

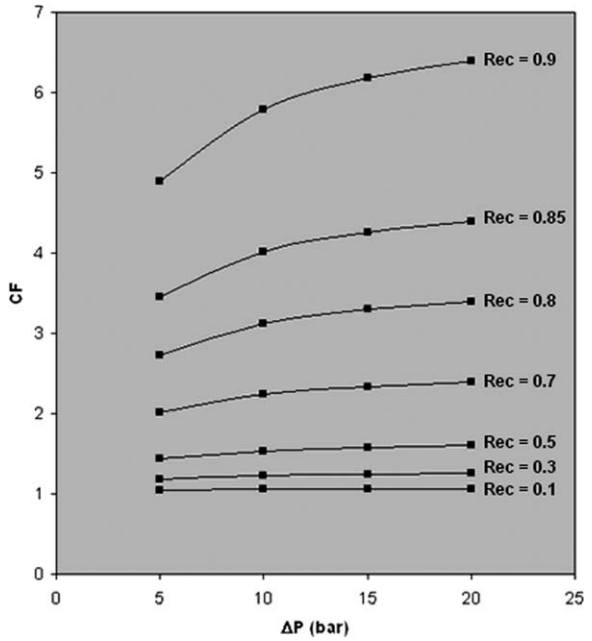

Figure 7. Evolution of the CF as function of the applied pressure and the recovery rate for a single-stage process.

solute, should be maintained low. If the direct relationship between the rejection coefficient of each solute and the applied pressure is kept in mind, the conflicting effects that the applied pressure produces become apparent. When the recovery rate tends to 0, the importance of the contribution by the rejection coefficients over the parameter is reduced, and under these conditions high pressures are preferred. On the other side, when the recovery rate tends to 1, the rejection coefficients gain more importance and the equilibrium between the values of each solute has to be balanced, resulting lower optimal pressures.

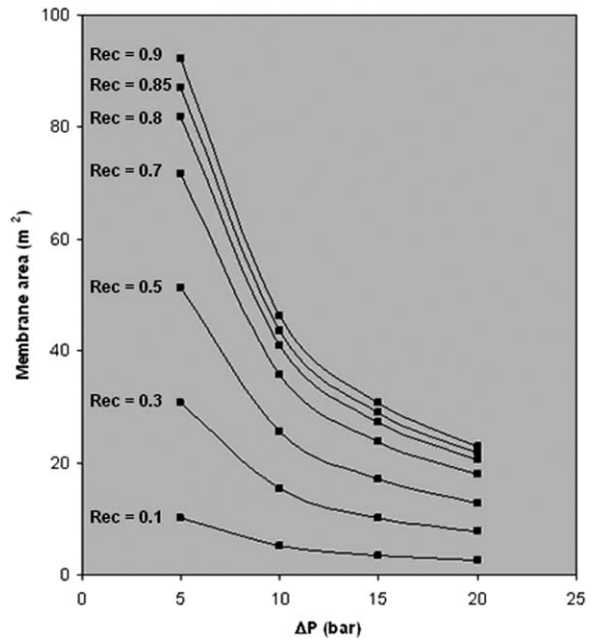

Figure 6. Evolution of the total membrane area as function of the applied pressure and the recovery rate for a single-stage process.

The influence of the recovery rate over the yield of the process has an opposite behavior (Figure 5): high recovery rates and the consequent high permeate streams imply low yields as an important part of the desired compound leaves the system after permeation through the membrane. Values higher than 95% can be obtained for a recovery rate of 0.1 but at the expense of a very poor purity. The maximum achievable yield for the maximum recovery rate, which corresponds to the optimum recovery rate to maximize the purity, is only 64% when the maximum pressure is applied. In this case, unlike for the purity, the optimal pressure is totally clear, as the maximum pressure assures the best yields for every recovery rate.

High pressures are also beneficial to decrease the required membrane area and to increase the CF for a constant recovery rate as it can be observed in Figures 6 and 7, respectively. The minimum membrane area corresponds to the lowest recovery rate. This result could be easily predicted as the permeate production is proportional to the membrane area. However, the maximum CF is achieved when the highest recovery rate is selected. This fact confirms the conflicting effects high recovery rates produce over the membrane system: while high purity and CF can be obtained when high pressures are applied, the counterpoint to these positive aspects is the poor yield of the process and the great membrane area that is necessary to work under these high-recovery conditions. On the contrary, the effects of the applied pressures are clearer, as high pressures are favourable in terms of process yield, membrane area, and CF (only the consequences over the product purity are not so positive as optimum values for this parameter require lower pressures).

Taking into account that the purity of the desired product and the process yield can be considered the two main parameters of the process, a further investigation was carried out to obtain a Pareto diagram interrelating both parameters using general algebraic modeling system (GAMS) as optimization software.

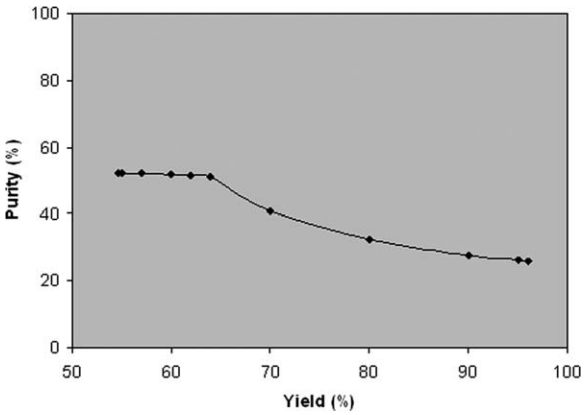

Figure 8. Pareto set of solutions including the product purity and the process yield for a single-stage process.

The GAMS is a high-level modeling system for mathematical programming and optimization. It consists of a language compiler and a stable of integrated high-performance solvers.[64]

The Pareto diagram of this problem that resulted from maximizing the purity of the product and the yield of the process simultaneously is depicted in Figure 8. A point in the Pareto frontier corresponds to the maximum feasible purity for a fixed yield and vice versa (the maximum feasible yield for a fixed purity). This type of multiobjective optimization can be formulated to maximize various variables, and in this case, it is solved by application of the epsilon constraint method. This method tackles multiobjective optimization problems by solving a series of single objective subproblems, where all but one objectives are transformed into constraints.[65–67]

The highest point on the left side represents the maximum product purity solution, and in an analogous way, the lowest point on the right side shows the maximum process yield. The left side of the frontier is characterized by a very flat plateau. This result means that only very little increases in the purity of the product can be obtained when the product purity is close to its maximum despite the great decreases in the yield of the process.

Analysis of the performance of the two-stage continuous process

After the analysis of the performance of a single-stage process, the cascade that incorporates two stages in the multistage continuous configuration (Figure 9) was investigated.

A sensitivity analysis was carried out to study the influence of the recovery rates of both stages over the system performance. The effects of varying the recovery rates in the range between 0.1 and 0.9 while keeping the applied pressures in both stages constant at 20 bar is graphed in Figure 10. Once again, the decision about the recovery rates should ride out the conflicting effects those variables produce over the process performance. The maximum achievable purity (higher than 78%) is obtained when the highest recovery rates are imposed to both stages. But this situation also implies the lowest process yield (only 53%). On the contrary, the maximum process yield (96%) can be attained by the application of the lowest recovery rates, resulting a product purity very close to the feed conditions (no higher than 27%).

A deeper look at the graphs in the Figure 10 can give an idea about the relative importance of the recovery rate in each stage. The process yield is clearly dominated by the value of this variable in the initial Stage 0: when the recovery rate in the Stage 0 is 0.1, the yield ranges between 94 and 96% for whichever value in the other stage, and this behavior is similar for the rest of the graph as indicated by the predominance of vertically oriented color zones (Figure 10b). It is obvious that a very low recovery rate in Stage 0 implies a very low permeate stream leaving this stage (and in this configuration also leaving the system), and consequently most of the desired product is maintained in the process and can be recovered in the final product stream even when high recovery rates are applied in the other stage. An equivalent reasoning can explain the low process yields when the recovery rate of the initial stage is 0.9 indistinctly of the final stage operation conditions. The prevalence of one stage does not occur in the case of product purity. For this parameter, both stages are relevant and high recovery rates in both of them are necessary to obtain high purity.

The situation that uses the highest total membrane area (more than 120 m^2) is the one corresponding to the recovery rate values of 0.1 in Stage 0 and 0.9 in Stage 1_{Rs}. The minimum recovery rate in the initial stage implies a high-flow retentate stream going to the second stage, and the maximum value in this latter stage produces a high-flow recirculation stream returning to the process. This way the high surface required by the second stage is justified by the combination of high-flow feed and permeate streams while the initial stage shows two counterbalancing effects: low recovery rate but high-flow feed stream as consequence of the recirculated stream. The opposite situation (lowest membrane area) coincides with the maximum process yield case, that is, minimum recovery rates in both stages and the consequent low membrane area, which can be enough to obtain low-flow permeate streams. A very insensitive zone can be found in the corresponding graph (Figure 10c) when the recovery rate in the final stage is 0.5. Under this condition, the value taken in the initial stage becomes unimportant as the total membrane area is maintained constant with a value very close to 25 m^2.

The CF was the last parameter investigated and it was found that its behavior is quite similar to the one of product purity, as its maximum value (48) is attained for the maximum recovery rates in both stages.

Comparison of three-stage cascades under multistage and dual continuous configurations

The dual cascade configuration requires at least three stages to be possible, so a comparison between a classical

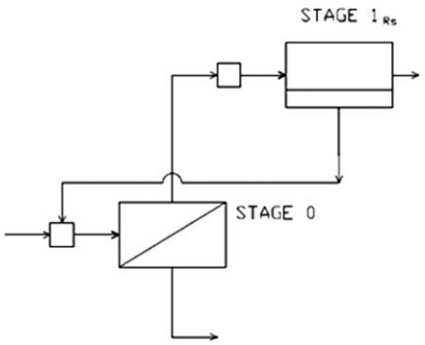

Figure 9. Two-stage cascade under multistage configuration.

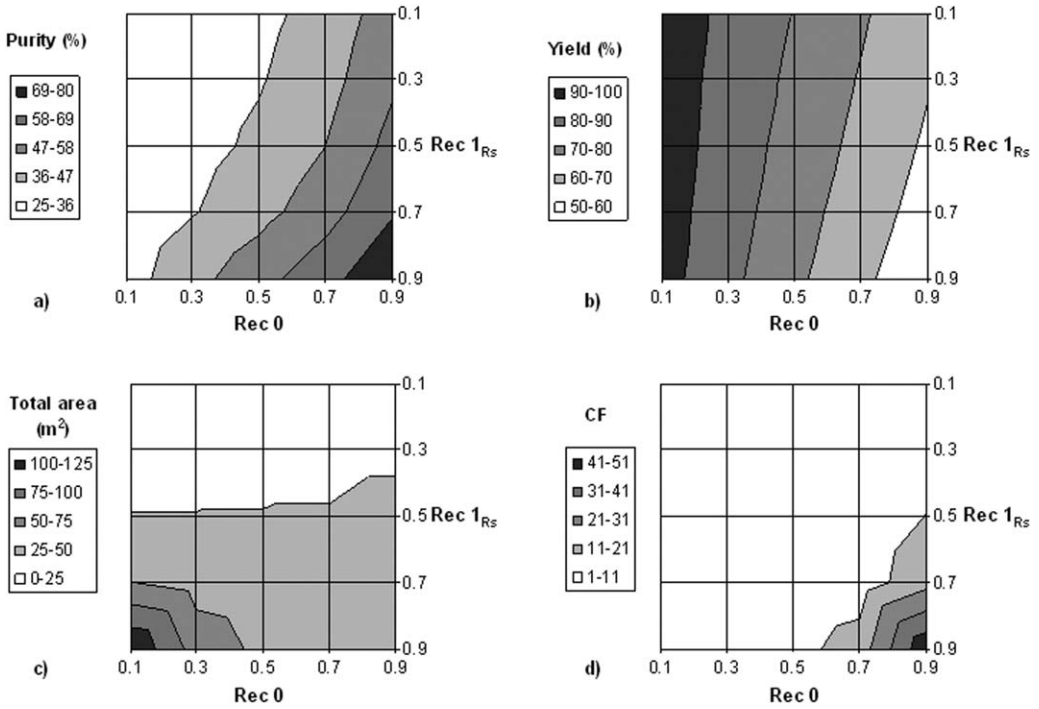

Figure 10. Evolution of the product purity (a), product yield (b), total membrane area (c), and CF (d) as function of the recovery rates for a two-stage process.

multistage cascade and a dual cascade (both of them comprising three stages) was carried out. Figure 11 shows the scheme of the multistage cascade, whereas the dual cascade is a particular case of the general scheme depicted in Figure 1 that results from consideration of an only module in each section (Stages 0, 1_{Ps}, and 1_{Rs}).

Once again, a sensitivity analysis was carried out to study the influence of the recovery rates of the different stages over the whole system performance. The applied pressures in every stage were maintained constant at 20 bar, whereas the values of the recovery rates were modified in the range between 0.1 and 0.9. As in this case there are three variables to investigate, it was decided to change the values of the extreme stages (Stages 0 and 2_{Rs} for the case of the multistage cascade and Stages 1_{Ps} and 1_{Rs} for the dual cascade) for three different values (0.1, 0.5, and 0.9) of the recovery rate of the central stage (Stage 1_{Rs} for the multistage configuration and Stage 0 for the dual configuration).

The evolution of the product purity can be observed in Figure 12. As expected, maximum purities correspond to maximum recovery rates, but great differences can be found between the configurations. The maximum achievable purity is obtained by the multistage cascade (93%), whereas the dual cascade can only attain a maximum value of 81%. The Stage 0 of the dual configuration is greatly important, as a low recovery rate in this stage implies low purity, which cannot be improved too much by the decisions taken about the other stages. Nevertheless, the multistage cascade has more potential to get better purity values after a low recovery rate in the feed stage by applying high recovery rates in the rest of the cascade.

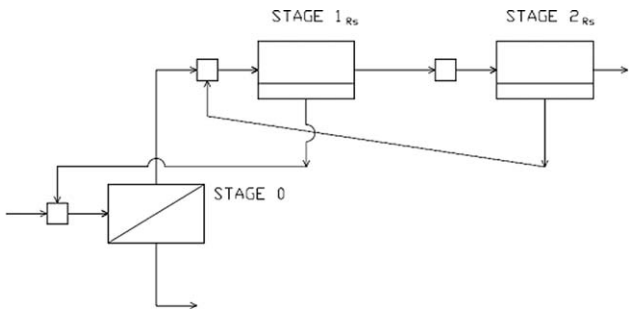

Figure 11. Three-stage cascade under multistage configuration.

The results about the process yield are contrary to those obtained for product purity and it can be seen in Figure 13. The maximum process yield is obtained by the dual cascade when works at the minimum recovery rates. Even the lowest process yield that can be found for the dual configuration is higher than 75% (corresponding to the maximum product purity situation). The maximum product purity result obtained by the multistage cascade at maximum recovery rates has to suffer a lower yield (below 50%).

To get more easily comparable results, it was decided to obtain the Pareto frontier that includes the product purity and the process yield for both configurations as it can be observed in Figure 14. It was decided to graph also the Pareto obtained for a single-stage process and the one corresponding to the two-stage configuration.

It is clear that the main advantage of the dual cascade is the upper yield it can achieve. For a particular product purity, the process yield is always higher when a dual cascade is used instead of a multistage cascade. This fact is limited to a purity value of 85%, as the dual cascade is very close to its upper limit and, for these cases, the multistage configuration should be preferred. When focusing on the multistage cascades, the addition of stages represents a great improvement of product purity, but it is very limited to improve the process yield.

The influence of the recovery rates over the resting parameters total membrane area and CF is depicted in Figures 15

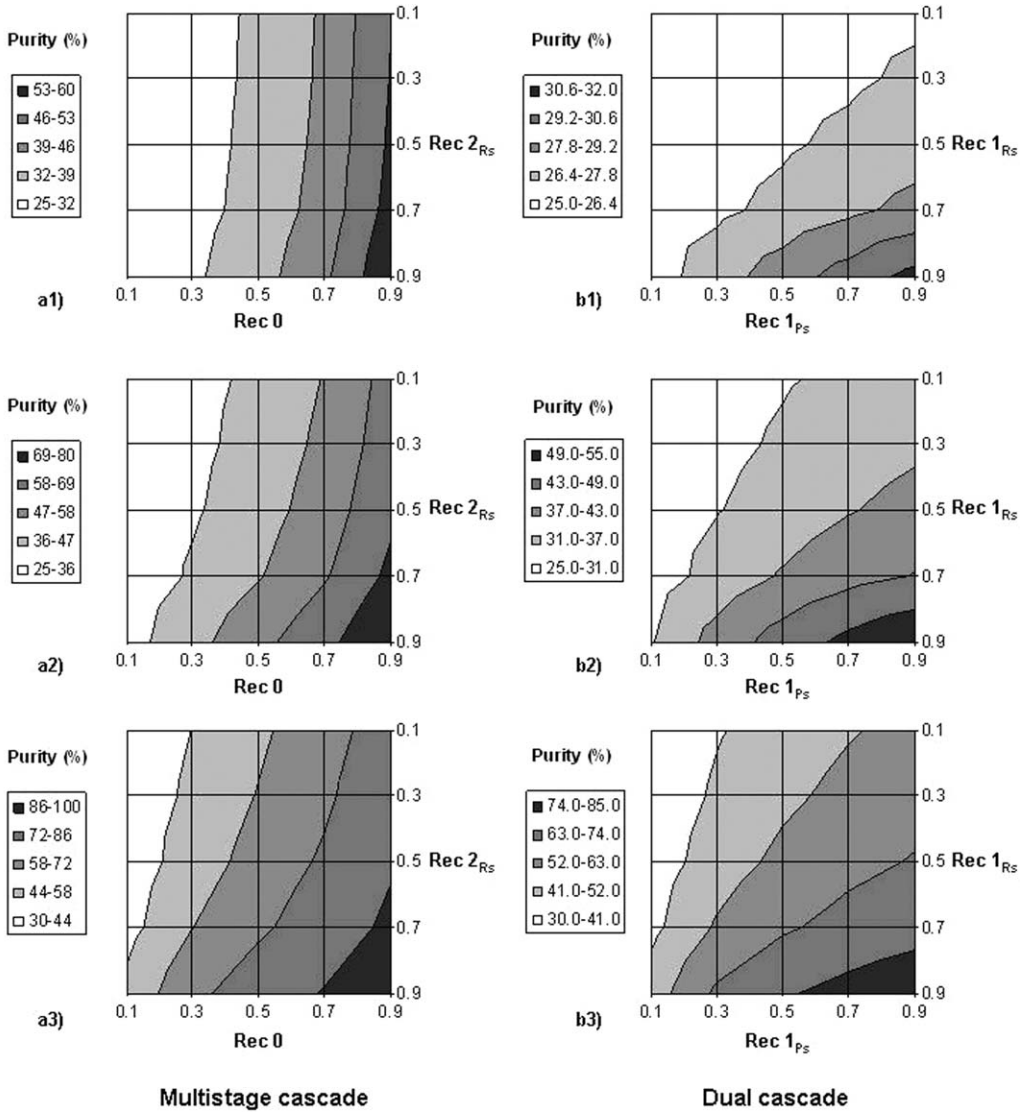

Figure 12. Evolution of the product purity for the three-stage multistage (a) and dual (b) cascades.

Numerical indexes indicate the value of the central recovery rate: 0.1 (1), 0.5 (2), and 0.9 (3).

and 16, respectively. In relation with the membrane area, it was found that both configurations have quite similar requirements and trends for this resource. If the maximum purity situation is taken as an example, the multistage cascade requires about 30 m^2 of membrane, whereas the dual cascade requires about 50 m^2.

The multistage cascade shows an apparent superiority above the dual configuration in another field that can be added to product purity: the CF. The multistage system is able to achieve a CF very close to 400, whereas the dual cascade can attain a factor of 63 (it is about the seventh part of the multistage value). These values have to be taken into account to consider that both types of cascades could be useful to concentrate solute present in very diluted streams. However, this fact may have some disadvantages related to the precipitation of solids as a consequence of the saturation of the streams above the corresponding solubility limits, or the appearance of new liquid phases when managing liquid solutes.

Dual cascades comprising four and five stages

To search the options of the dual cascades performance that combine product purity and process yield in a better way, further advances in the analysis of this type of cascades were performed. Figure 17 shows the Pareto frontiers for the dual cascades comprising four and five stages, where it is observed that values of purity and yield of nearly 100% can be achieved.

For the case of the four-stage cascade, the configuration that includes two stages in the retentate side and one stage in the permeate side (2R1P), and the cascade that includes only a stage in the retentate side and two stages in the permeate side (1R2P) were taken under consideration. Two different configurations of five-stage cascades were considered: the one including three stages in the retentate side (3R1P) and a unique stage in the permeate side, and the one combining two stages in each side (2R2P). The five-stage integrating one stage in the retentate side and three stages in the permeate side (1R3P) was discarded as it is not pointed to the purification of the most retained solute. The obtained results were also compared with the simplest dual cascade composed by three stages.

The comparison between both four-stage cascades shows the advantages of choosing the 2R1P configuration. This scheme implies a higher maximum purity, while the maximum

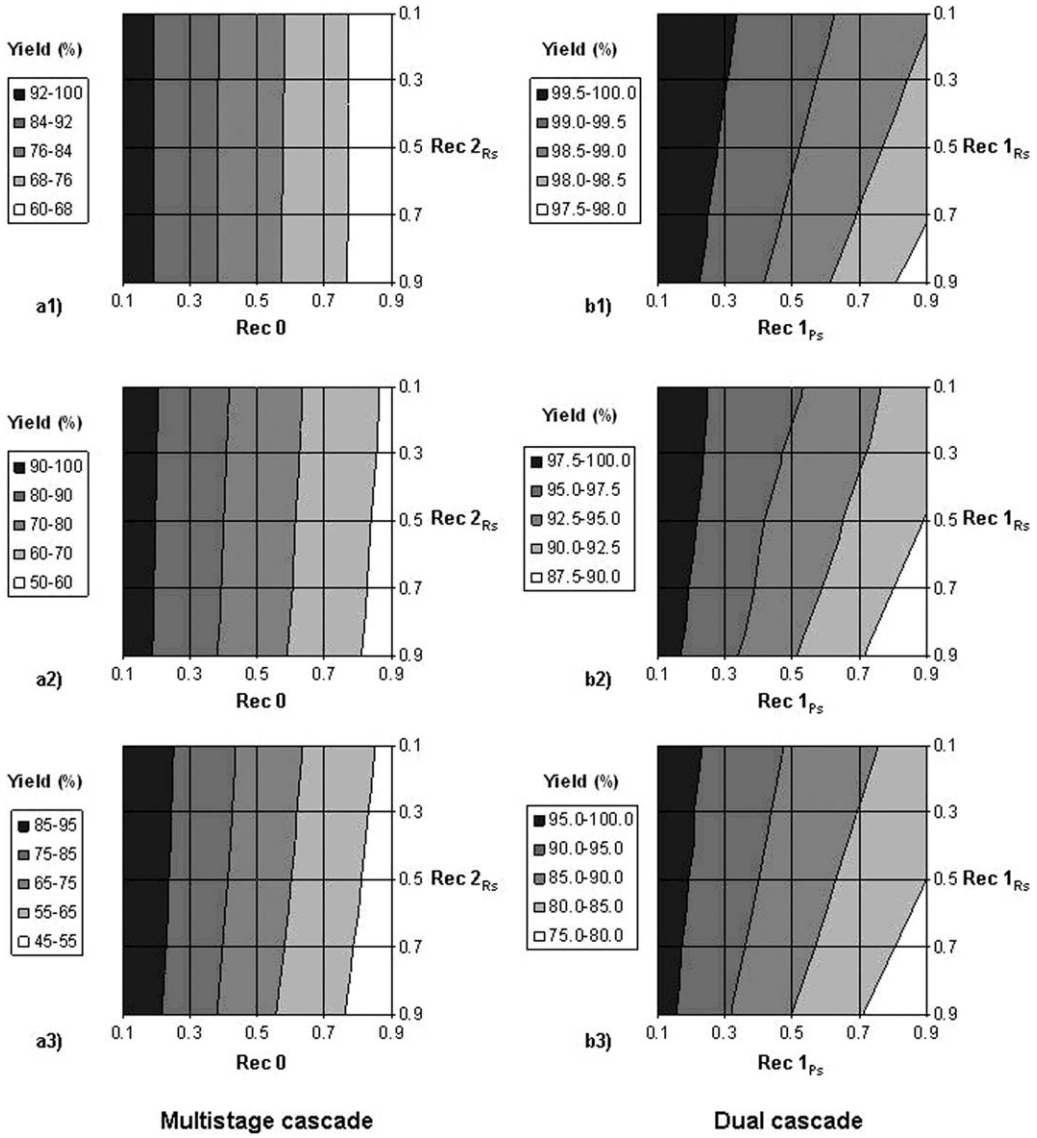

Figure 13. Evolution of the process yield for the three-stage multistage (a) and dual (b) cascades.

Numerical indexes indicate the value of the central recovery rate: 0.1 (1), 0.5 (2), and 0.9 (3).

purity achievable by the 1R2P configuration is quite close to the one achievable by the three-stage cascade. The 1R2P cascade is able to improve the results of the 2R1P configuration only for product purity values lower 80%, as it can get the same purity with a higher process yield.

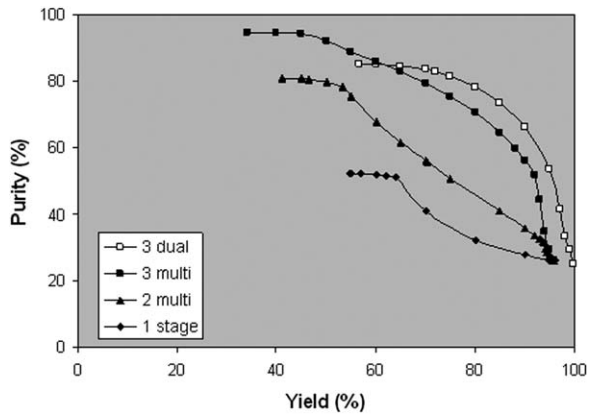

Figure 14. Pareto set of solutions including the product purity and the process yield for several process configurations.

The results of the five-stage cascades are quite similar. As it could be expected, the 3R1P configuration is a bit more effective for high product purity, but the 2R2P configuration can be more adequate to increase the process yield.

Optimal dual cascades: economic evaluation

An optimization problem was proposed to be able to quantify the differences in the cascades performance in economic terms. By implementation of the proposed simulation model, the behavior of the membrane cascades for continuous operation can be studied, and the corresponding economic trends can be investigated. The optimum operation conditions that would minimize the TC of the process can be obtained in a easy way by applying an optimization routine.[68]

The TC, defined by Eq. 25, were chosen as the formulated objective function to minimize. All the model variables have been expressed in terms of the operation variables (recovery rates and applied pressures). The constraints for these independent variables have been set as gathered in Table 3. The

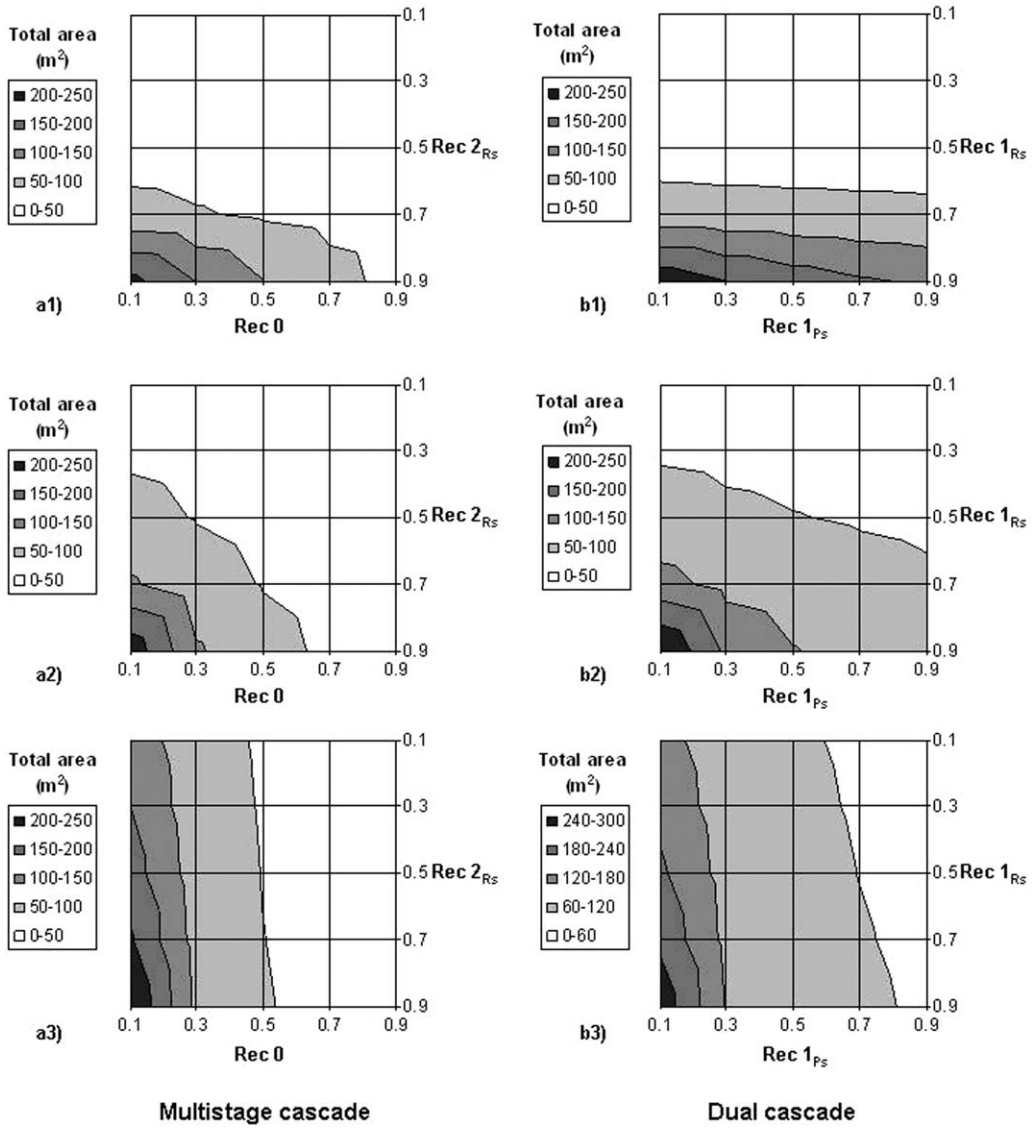

Figure 15. Evolution of the total membrane area for the three-stage multistage (a) and dual (b) cascades.

Numerical indexes indicate the value of the central recovery rate: 0.1 (1), 0.5 (2), and 0.9 (3).

valid interval of the recovery rate was defined from 0.1 to 0.9 taking into account that recovery rates close to 1 may cause problems of polarization, and recovery rate values close to 0 imply very high concentrations of solutes in the retentate stream. Related to the pressure range, it has been chosen to operate under safe conditions taking into account the maximum pressure recommended by the membrane manufacturers. Another constraint was added to include the product specifications. In this case, product purity was considered the limiting factor, so a minimum value that must be achieved has to be fixed (90% purity was selected).

The feed conditions that were proposed for the simulation cases (that is, 1 m^3/h with solute concentrations of 25 and 75 ppm for Compounds A and I, respectively) were also assumed for this optimization problem. Information about the values for all the parameters appearing in the economic model can be observed in Table 4. The lifetime of the membrane was assumed to be 2 years, whereas the rest of the installation was designed to last for 10 years. The price of the Organic Solvent Nanofiltration (OSN) membranes is located within the range proposed by other authors.[4,36] The Compound A price is 1600$/kg, so it was assumed that the lost chemical cannot be so valuable as it is not in a purified form. This way, half of the price of the pure compound was assigned as chemical loss cost.

GAMS software was selected as optimization tool to manage the resulted nonlinear programming model using CONOPT3 solver.

The technical aspects of the optimization of the most interesting configurations of dual membrane cascades (2R1P, 3R1P, and 2R2P) are compared in Table 5, and the corresponding economic results appear in Table 6. The 3R1P cascade gives the best economic results as it is characterized by the minimum TC among all the options, but the 2R1P is really close (only 3 $/d of difference between both configurations). This scarce margin can be explained by the lower OC of a five-stage cascade when compared with a four-stage one, this latter implying higher chemical losses (73.6% process yield vs. 73.9% for the five-stage case) and more flow in the residual stream that has to be treated. The lower CC required by the four stages as consequence of less total membrane area cannot compensate the additional OC. The other proposed

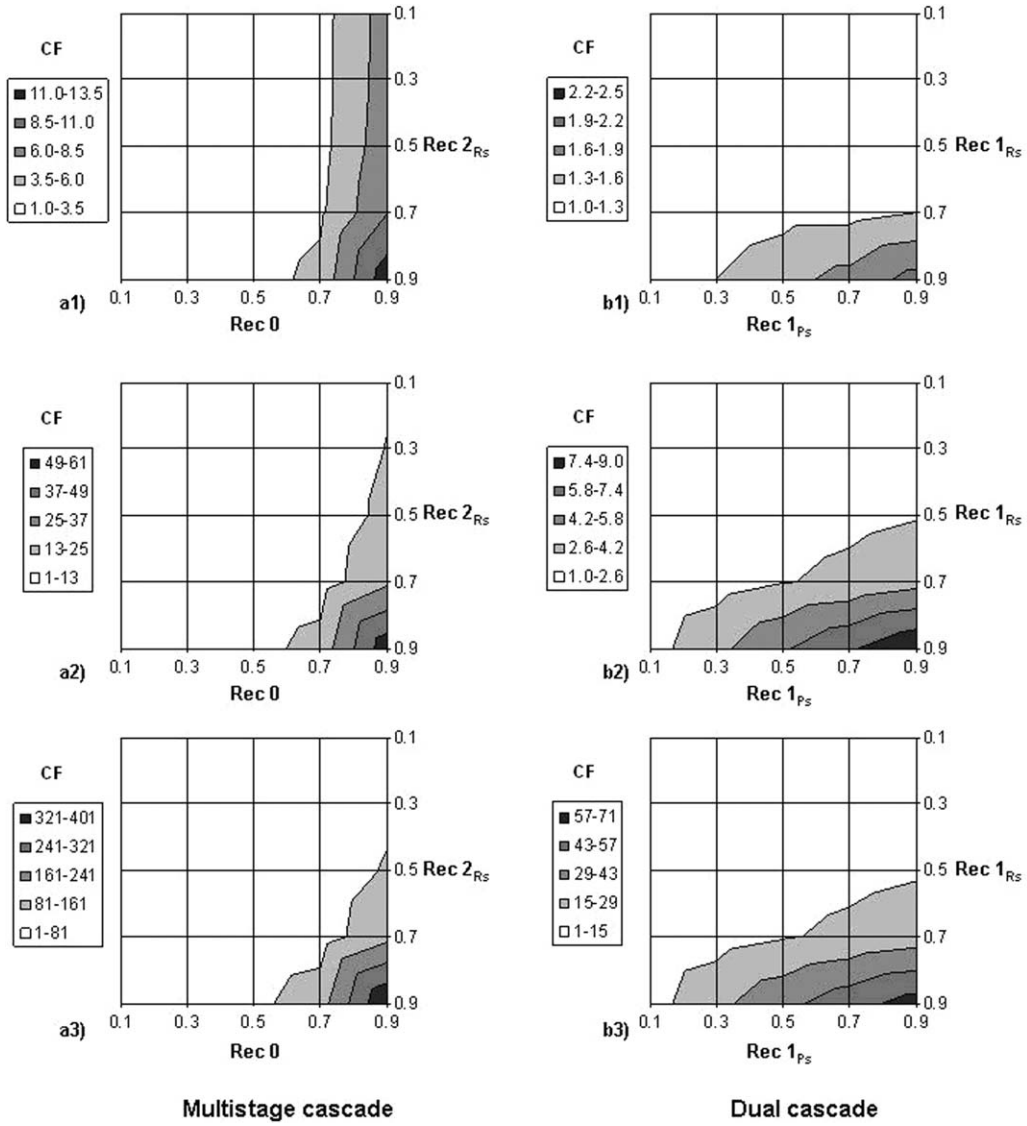

Figure 16. Evolution of the CF for the three-stage multistage (a) and dual (b) cascades.

Numerical indexes indicate the value of the central recovery rate: 0.1 (1), 0.5 (2), and 0.9 (3).

cascade is not so far: the difference is 656 $/d when compared to the optimal result, which represents an increase of the total cost lower than 4%. In this case, the 2R2P cascade shows the highest process yield (a value of 85.8%) and it can reduce the operating costs mainly because of this reduction of the chemical loss, but at expenses of the highest CC caused by the necessity of higher membrane area.

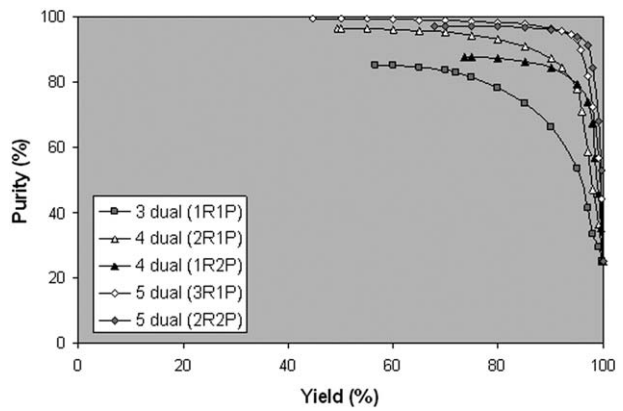

Figure 17. Pareto set of solutions including the product purity and the process yield for dual cascades composed by three, four, and five stages.

As it is observed from the optimization results, the main cost of the process is the treatment of the residual stream leaving the system. It represents as much as 90% of the TC for the optimal 3R1P situation and more than 85% for the 2R2P cascade, which is the one with the lowest contribution. It is clear that this process can only be considered as a viable option when the solvent recovery from the residual stream leaving the system is incorporated.

A brief commentary about the optimal operation conditions is presented. The applied pressures tend to take the

Table 3. Optimization Problem Formulation

Objective Function	TC in Eq. (X)
Optimization target	Minimize
Independent variables	$\mathrm{Rec}(i)$, $\Delta P(i)$
Constraints to independent variables	$0.1 < \mathrm{Rec}(i) < 0.9$
	$5\ \mathrm{bar} < \Delta P(i) < 20\ \mathrm{bar}$
Other constraints	Purity > 90%

Table 4. Economic Model Parameters

Parameter	Unit	Value
LT_{memb}	d	730
LT_{inst}	d	3650
Y_{memb}	$/m^2	2000
Y_{sal}	$/h	10
Y_{elec}	$/kWh	0.08
Y_{loss}	$/kg	800
Y_{waste}	$/m^3	670
η		0.70

maximum value that has been fixed (only the 2_{Ps} stage in the 2R2P cascade works at a pressure different from 20 bar, but it is very close as its value is 19.6 bar) even when the stages work at high recovery rates inspite of the fact that the single-stage simulations demonstrated the option to reach higher purity values by applying lower pressures. With respect to the recovery rates, their optimal values depend on the position of the stage. The feed stage and all the stages in the permeate side of the cascade work at the maximum allowed recovery rate, but the stages in the retentate side takes value below the upper limit: the farther away from the feed stage, the lower the optimal recovery rate.

The influence of the desired product purity over the performance of the two most competitive cascades (2R1P and 3R1P) was analyzed. In this case, the product purity constraint was modified to increase the required product purity to a value of 95%. The main optimization results (technical aspects and economic terms) are shown in Tables 7 and 8, respectively.

As expected, an increase in the demanded purity involves higher TC, but this rise is smaller for the five-stage configuration (less than a 5% increase while the four-stage cascade suffers a 7% rise). This difference between the TC demonstrated that the four-stage cascade has greater difficulties to compete with the five-stage configuration when more exigent purity requirements are imposed, mainly because of the lower process yield that entails larger amount of chemical loss. Moreover, the necessity of high recovery rates (all the stages in the 2R1P cascade need 0.9 recovery rates) implies larger membrane area, and although having one stage more, the five-stage cascade can work with a lower total membrane area and the consequent lower CC.

Table 5. Optimization Technical Results

	Four Stages (2R1P)	Five Stages (3R1P)	Five Stages (2R2P)
Recovery rates			
Rec0	0.90	0.90	0.90
$Rec1_{Rs}$	0.87	0.84	0.86
$Rec2_{Rs}$	0.77	0.70	0.75
$Rec3_{Rs}$		0.42	
$Rec1_{Ps}$	0.90	0.90	0.90
$Rec2_{Ps}$			0.90
Applied pressures (bar)			
$\Delta P0$	20.0	20.0	20.0
$\Delta P1_{Rs}$	20.0	20.0	20.0
$\Delta P2_{Rs}$	20.0	20.0	20.0
$\Delta P3_{Rs}$		20.0	
$\Delta P1_{Ps}$	20.0	20.0	20.0
$\Delta P2_{Ps}$			19.6
Membrane area (m^2)			
$A0$	28.3	28.3	28.6
$A1_{Rs}$	3.0	3.0	3.0
$A2_{Rs}$	0.4	0.5	0.4
$A3_{Rs}$		0.1	
$A1_{Ps}$	25.5	25.5	28.3
$A2_{Ps}$			25.5
Product purity (%)	90.0	90.0	90.0
Process yield (%)	73.6	73.9	85.8
CF	178	164	171

Table 6. Economic Breakdown of the Optimal Cascades

Costs ($/d)	Four Stages (2R1P)	Five Stages (3R1P)	Five Stages (2R2P)
TC	17,832	17,829	18,485
CC	1379	1383	2068
CC_{memb}	157	157	235
CC_{inst}	1222	1226	1833
OC	16,452	16,446	16,416
OC_{en}	4	4	6
OC_{lab}	240	240	240
OC_{m}	69	69	103
OC_{loss}	127	125	68
OC_{waste}	16,013	16,008	15,999

Optimal dual cascades with solvent recovery: configurations and economic evaluation

As it was mentioned in the previous section, the economic considerations of this process force to take into account the recovery of the great amount of solvent that leaves the system by the permeate side of the cascade. Organic solvents usage efficiency in the pharmaceutical industry has much room for improvement, and increasing solvent recovery and recycling rates have to be part of the implemented optimal strategies to reduce solvent wastage.[15]

In this case, the installation of a solvent resistant reverse osmosis unit after the last stage of the permeate side of the cascade was designed according to the scheme seen in Figure 18. The performance of this reverse osmosis stage is characterized by a lower solvent permeation when compared with the nanofiltration membranes (45% reduction in terms of the membrane permeability) and a higher retention of both solutes (the value of the rejection coefficients for both solutes is 0.995 at 35 bar). This way, the stream leaving the

Table 7. Optimization Technical Results for More Exigent Purity Requirement

	Four Stages (2R1P)	Four Stages (2R1P)	Five Stages (3R1P)	Five Stages (3R1P)
	90% Purity	95% Purity	90% Purity	95% Purity
Recovery rates				
Rec0	0.90	0.90	0.90	0.90
$Rec1_{Rs}$	0.87	0.90	0.84	0.84
$Rec2_{Rs}$	0.77	0.90	0.70	0.76
$Rec3_{Rs}$			0.42	0.68
$Rec1_{Ps}$	0.90	0.90	0.90	0.90
Applied pressures				
$\Delta P0$	20.0	20.0	20.0	20.0
$\Delta P1_{Rs}$	20.0	20.0	20.0	20.0
$\Delta P2_{Rs}$	20.0	6.0	20.0	20.0
$\Delta P3_{Rs}$			20.0	20.0
$\Delta P1_{Ps}$	20.0	20.0	20.0	20.0
Membrane area				
$A0$	28.3	28.4	28.3	28.4
$A1_{Rs}$	3.0	3.1	3.0	3.1
$A2_{Rs}$	0.4	1.0	0.5	0.3
$A3_{Rs}$			0.1	0.1
$A1_{Ps}$	25.5	25.6	25.5	25.6
Product purity	90.0	95.0	90.0	95.0
Process yield	73.6	70.2	73.9	72.2
CF	178	518	164	576

Table 8. Economic Breakdown of the Optimal Cascades for more Exigent Purity Requirement

Costs ($/d)	Four Stages (2R1P) 90% Purity	Four Stages (2R1P) 95% Purity	Five Stages (3R1P) 90% Purity	Five Stages (3R1P) 95% Purity
TC	17,832	17,916	17,829	17,892
CC	1379	1401	1383	1385
CC_{memb}	157	159	157	157
CC_{inst}	1222	1242	1226	1228
OC	16,452	16,515	16,446	16,506
OC_{en}	4	4	4	4
OC_{lab}	240	240	240	240
OC_m	69	70	69	69
OC_{loss}	127	143	125	134
OC_{waste}	16,013	16,058	16,008	16,060

permeate side of the cascade can be purified to recover solvent with very low solute content. A new process parameter (called recovery) can be defined to evaluate the amount of solvent that is recovered

$$\text{Recovery } = 100\frac{Q_{\text{solv}}}{F} \tag{37}$$

The inclusion of the solvent recovery stage implies some modifications of the proposed economic model. The stream that has to be treated as waste changes, and in this situation, it is the one that leaves the reverse osmosis unit as retentate

$$\text{OC}_{\text{waste}} = Q_{\text{waste}} \cdot Y_{\text{waste}} \tag{38}$$

Moreover, a new stream has to be taken under consideration: the permeate of the reverse osmosis unit is a valuable stream of recovered solvent and it brings a money save as its recycling allows a decrease in the solvent consumption of the whole downstreaming process

$$C_{\text{solv}} = Q_{\text{solv}} \cdot Y_{\text{solv}} \tag{39}$$

where C_{solv} is the money save attributable to the recovered solvent, and Y_{solv} is the price of the solvent (in this case 250 $\$/m^3$). To contrast this new money save to the TC of the process, it was decided to define the economic profit Z as the difference between these two terms

$$Z = C_{\text{solv}} - \text{TC} \tag{40}$$

The economic profit was considered as the maximization target for the optimization of the installations with integration of solvent recovery. The applied pressure in the reverse osmosis unit was not subject to optimization, and the maximum allowed value, that is 35 bar, was fixed.

The required product purity was imposed to be at least 95%, as it was demonstrated previously, the increase from 90 to 95% does not imply excessive extra costs for the 2R1P and 3R1P cascades. New constraints expressed as solute limits were included to control the quality of the recovered solvent. The optimization results that correspond to the case that limits the maximum solute concentration in the recovered solvent to 40 ppb are shown in Tables 9 and 10 for the technical aspects and economic terms, respectively.

Tables 9 and 10 also include the results for cases with lower solute limits for the solvent (2 and 1 ppb), but these situations cannot be achieved by a unique reverse osmosis unit, so a second unit was added in series with the previous one as shown in Figure 19. The joint of these two stages including the recirculation between them can be considered as a two-stage multipass cascade, and more stages following this configuration could be added to attain higher solvent quality.

The analysis of the process recoveries shows that, even for the most exigent conditions, more than 80% of the solvent that enters the process can be recovered, with a value very close to 90% for the least strict situation. The solvent recovery stages do not produce important interferences over the rest of the cascade as similar process yields are obtained (only a reduction of 0.2% for the 3R1P cascade when incorporates two reverse osmosis units can be identified). The fact that the operation conditions of the optimal cascades incorporating the solvent recovery system are not too different from the ones obtained without the solvent recovery confirms that the consideration of solvent recovery does not imply technical disadvantages.

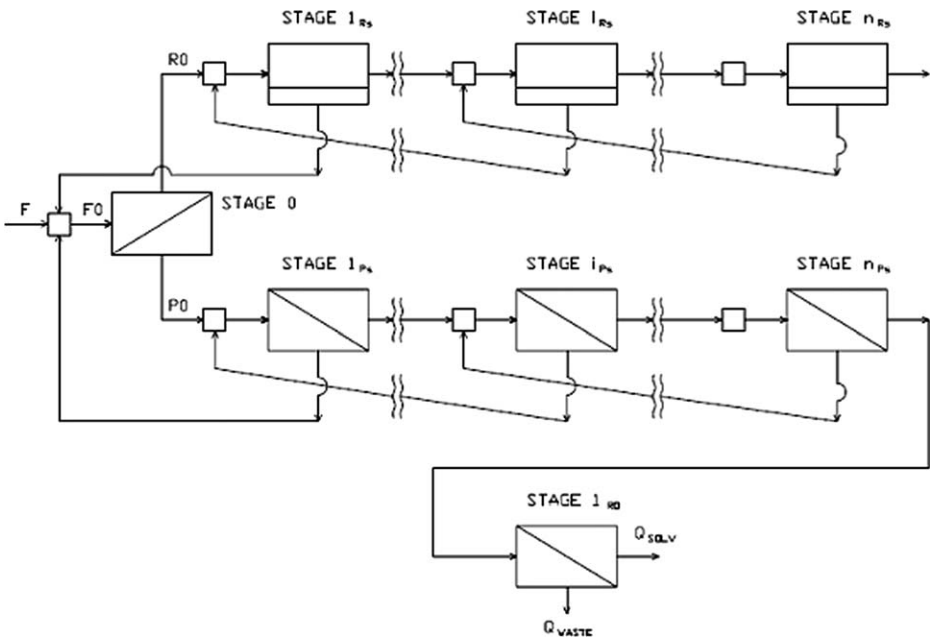

Figure 18. General scheme of a dual membrane cascade including one stage for solvent recovery.

Table 9. Optimization Technical Results for Solvent Recovery

	Four Stages (2R1P)			Five Stages (3R1P)		
Limit for the recovered solvent (ppb)	40	2	1	40	2	1
Recovery rates						
Rec0	0.90	0.90	0.90	0.90	0.90	0.90
$Rec1_{Rs}$	0.90	0.90	0.90	0.90	0.90	0.90
$Rec2_{Rs}$	0.90	0.90	0.90	0.62	0.68	0.90
$Rec3_{Rs}$				0.86	0.10	0.27
$Rec1_{Ps}$	0.90	0.90	0.90	0.90	0.90	0.90
Rec1RO	0.90	0.90	0.90	0.90	0.90	0.90
Rec2RO		0.90	0.49		0.90	0.49
Applied pressures						
$\Delta P0$	20.0	20.0	20.0	20.0	20.0	20.0
$\Delta P1_{Rs}$	20.0	20.0	20.0	20.0	20.0	20.0
$\Delta P2_{Rs}$	6.0	6.0	6.0	20.0	20.0	20.0
$\Delta P3_{Rs}$				20.0	20.0	20.0
$\Delta P1_{Ps}$	20.0	20.0	20.0	20.0	20.0	20.0
$\Delta P1RO$	35.0	35.0	35.0	35.0	35.0	35.0
$\Delta P2RO$		35.0	35.0		35.0	35.0
Membrane area						
$A0$	28.4	28.4	28.4	28.4	28.4	28.4
$A1_{Rs}$	3.1	3.1	3.1	3.1	3.1	3.1
$A2_{Rs}$	1.0	1.0	1.0	0.3	0.3	0.3
$A3_{Rs}$				0.2	0.1	0.1
$A1_{Ps}$	25.6	25.6	25.6	25.6	25.6	25.6
$A1RO$	23.9	26.3	44.5	23.9	26.3	44.5
$A2RO$		23.6	21.6		23.6	21.6
Product purity	95.0	95.0	95.0	95.0	95.0	95.0
Process yield	70.2	70.2	70.2	72.8	72.0	72.0
CF	518	518	518	674	707	707
Recovery	89.9	88.9	81.3	89.9	88.9	81.3

Table 10. Economic Breakdown of the Optimal Cascades for Solvent Recovery

Costs ($/d)	Four Stages (2R1P)			Five Stages (3R1P)		
Limit for the recovered solvent (ppb)	40	2	1	40	2	1
TC	4071	4891	6532	4046	4866	6505
CC	1977	2604	2995	1964	2588	2978
CC_{memb}	225	296	340	223	294	338
CC_{INST}	1752	2308	2654	1741	2293	2640
OC	2094	2287	3537	2081	2277	3526
OC_{en}	6	9	13	6	9	13
OC_{lab}	240	240	240	240	240	240
OC_{m}	99	130	150	98	129	149
OC_{loss}	143	143	143	131	134	134
OC_{waste}	1606	1765	2991	1606	1765	2990
C_{solv}	5393	5333	4876	5394	5335	4878
Z	1322	442	−1656	1348	469	−1627

The economic aspects of the solvent recovery are more significant. The decrease in the flow of the stream to be treated suppose a great decrease in the TC of the system: the reduction ranges from 64 to 77% for both cascades depending on the required solvent quality (solute limits of 1 ppb and 40 ppb, respectively). This way, it is clear that the influence over the waste treatment costs compensates the higher membrane area required by the additional stages (the price and lifetime of the reverse osmosis membranes were assumed equal to the ones of the nanofiltration membranes). However, the most decisive economic aspect is the save in raw solvent that can be achieved by recycling the recovered stream. This way, the cascade can obtain a positive economic profit when the quality requirements imposed to the solvent are not too exigent (limit concentrations higher than 1 ppb), as the solvent save can recompense the TC of the installations.

Conclusions

Multiple configurations of organic solvent nanofiltration membrane cascades can be considered and the final establishment of each design would depend on the specific separation targets. In this article, the configurations analyzed for the proposed separation process were the multistage cascades up to three stages, and the dual membrane cascades comprising multistage and multipass sections up to five stages in total.

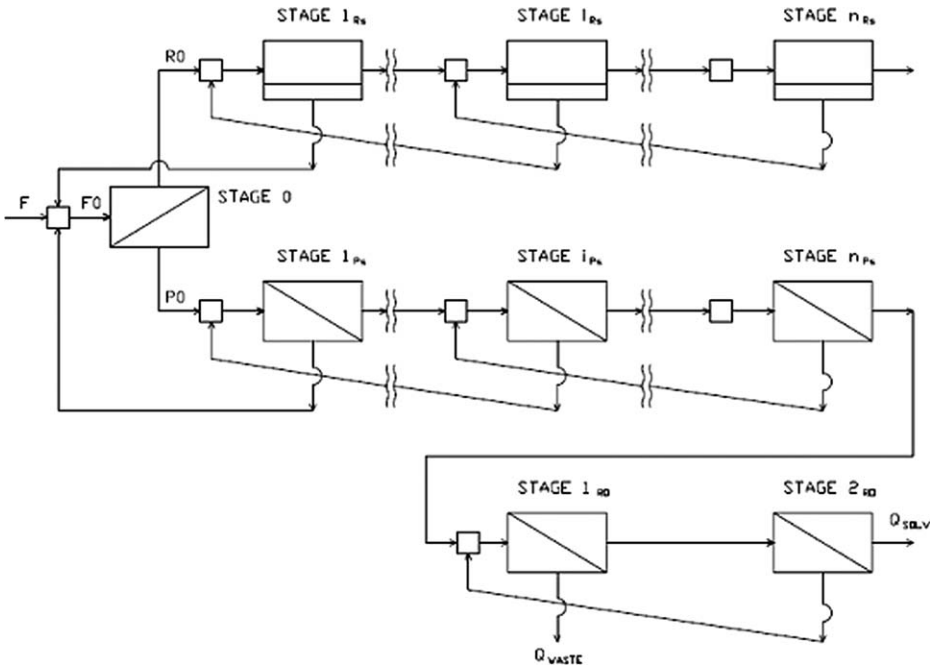

Figure 19. General scheme of a dual membrane cascade including two stages for solvent recovery.

A simulation model based on the equations for solvent and solute transport through the membranes and the mass balances (overall and by components) was formulated to represent the process (membrane modules and mixers), and some sensitivity analyses were performed to evaluate the performance of the systems.

The Pareto diagrams were used to interrelate the two main variables for the production process: the purity of the desired product and the process yield. From the Pareto set of solutions, the scenarios to maximize both variables were identified, and the obtained results for the dual cascades comprising four and five stages show the points where the maximum values, nearly 100%, can be achieved for the product purity and the process yield.

The economic evaluation of different configurations was also performed. The TC were chosen as the formulated objective function to minimize in the economic optimization strategy, with the operation variables (recovery rates and pressures) as independent variables and under the consideration of product specifications (product purity) as restrictions. As it is observed from the optimization results, the main cost of the process is the treatment of the residual stream leaving the system. It represents more than 85% for the dual cascades. It is pointed out that this process can only be considered as a viable option when the solvent recovery from the residual stream leaving the system is incorporated.

For the solvent recovery, reverse osmosis modules were added to the last stage of the permeate side of the dual cascades of four and five stages. The inclusion of the solvent recovery system implied some modifications of the proposed economic model in the objective function, and new constraints expressed as solute limits to control the quality of the recovered solvent. The reduction of the TC of the considered systems was significant: 64–77% depending on the required solvent quality (1 and 40 ppb, respectively).The solvent recovery influence over the waste treatment costs compensates the higher membrane area required for the installation when the additional recovery unit is included for solvent recovery.

Acknowledgments

This research has been financially supported by the Ministry of Science and Innovation of Spain (MICINN) through the projects CTQ2010-16608 and ENE2010-14828

Notation

A = membrane area, m^2
CC = capital costs, \$/d
CC_{inst} = capital costs attributable to installation, \$/d
CC_{memb} = capital costs attributable to membranes, \$/d
CF = concentration factor
cF^{sol} = solute concentration on the feed stream, ppm
cP^{sol} = solute concentration on the permeate stream, ppm
cR^{sol} = solute concentration on the retentate stream, ppm
C_{solv} = save due to solvent recovery, \$/d
F = feed stream flow, m^3/d
$(C_S)_{ln}$ = logarithmic average solute concentration across the membrane, mol/m^3
J^{sol} = flux of the solute due to the gradient of chemical potential, mol/m^2 d
J_V = permeate flux, m/d
K_{memb} = ratio membrane capital costs to total capital costs
L_P = hydraulic permeability coefficient, m/d bar
LT_{inst} = installation lifetime, d
LT_{memb} = membrane lifetime, d
OC = operation costs, \$/d
OC_{en} = energy costs, \$/d
OC_{lab} = labor costs, \$/d
OC_{loss} = chemical losses costs, \$/d
OC_m = maintenance costs, \$/d
OC_{waste} = waste treatment costs, \$/d
P = permeate stream flow, m^3/d
Q_{solv} = flux of recovered solvent, m^3/d
Q_{waste} = flux of waste stream after solvent recovery, m^3/d
R = retentate stream flow, m^3/d
R^{sol} = solute rejection coefficient
Rec = stage recovery rate
TC = total costs, \$/d
Y_{elec} = electricity price, \$/kWh
Y_{loss} = lost chemical price, \$/kg
Y_{memb} = price of solvent resistant membranes, $\$/m^2$
Y_{sal} = salary, \$/h
Y_{solv} = solvent price, $\$/m^3$
Y_{waste} = waste treatment cost, $\$/m^3$
Z = economic profit, \$/d

Greek letters

ΔC^{sol} = solute concentration difference across the membrane, mol/m^3
ΔP = pressure difference across the membrane, bar
η = pump efficiency
σ^{sol} = solute reflection coefficient
ω^{sol} = modified coefficient of solute permeability, m/d

Subscripts

Ps = permeate section of the dual cascade
Rs = retentate section of the dual cascade

Literature Cited

1. Doelle HW, Fiechter A, Schlegel G, Shimizu S, Ulber R, Yamada H. Biotechnology, 4. Downstream processing. *Ullmann's Encyclopedia of Industrial Chemistry, Electronic Release*. Weinheim: Wiley-VCH, 2009.
2. Degerman M, Jakobsson N, Nilsson B. Designing robust preparative purification processes with high performance. *Chem Eng Technol.* 2008;31:875–882.
3. Siew WE, Livingston AG, Ates C, Merschaert A. Continuous solute fractionation with membrane cascades–a high productivity alternative to diafiltration. *Sep Purif Technol*. 2013;102:1–14.
4. Székely G, Gil M, Sellergren B, Heggie W, Ferreira FC. Environmental and economic analysis for selection and engineering sustainable API degenotoxification processes. *Green Chem.* 2003;15:210–225.
5. van Reis R, Zydney A. Bioprocess membrane technology. *J Membr Sci*. 2007;297:16–50.
6. Grote F, Fröhlich H, Strube J. Integration of ultrafiltration unit operations in biotechnology process design. *Chem Eng Technol*. 2011;34: 673–687.
7. Rathore AS, Shirke A. Recent developments in membrane-based separations in biotechnology processes: review. *Prep Biochem Biotechnol*. 2011;41:398–421.
8. Grote F, Fröhlich H, Strube J. Integration of reverse-osmosis unit operations in biotechnology process design. *Chem Eng Technol.* 2012;35:191–197.
9. White LS. Development of large-scale applications in organic solvent nanofiltration and pervaporation for chemical and refining processes. *J Membr Sci*. 2006;286:26–35.
10. Pink CJ, Wong HT, Ferreira FC, Livingston AG. Organic solvent nanofiltration and adsorbents: a hybrid approach to achieve ultra low palladium contamination of post coupling reaction products. *Org Process Res Dev*. 2008;12:589–595.
11. So S, Peeva LG, Tate EW, Leatherbarrow RJ, Livingston AG. Organic solvent nanofiltration: a new paradigm in peptide synthesis. *Org Process Res Dev*. 2010;14:1313–1325.
12. Darvishmanesh S, Firoozpour L, Vanneste J, Luis P, Degrève J, van der Bruggen B. Performance of solvent resistant nanofiltration membranes for purification of residual solvent in the pharmaceutical

industry: experiments and simulation. *Green Chem.* 2011;12: 3476–3483.
13. Tylkowski B, Tsibranska I, Kochanov R, Peev G, Giamberini M. Concentration of biologically active compounds extracted from *Sideritis ssp. L. by nanofiltration. Food Bioprod Process.* 2011;89:307–314.
14. Abels C, Redepenning C, Moll A, Melin T, Wessling M. Simple purification of ionic liquid solvents by nanofiltration in biorefining of lignocellulosic substrates. *J Membr Sci.* 2012;405–406:1–10.
15. Siew WE, Livingston AG, Ates C, Merschaert A. Molecular separation with an organic solvent nanofiltration cascade–augmenting membrane selectivity with process engineering. *Chem Eng Sci.* 2013;90:299–310.
16. Jiménez-González C, Poechlauer P, Broxterman QB, Yang BS, am Ende D, Baird J, Bertsch C, Hannah RE, Dell'Orco P, Noorman H, Yee S, Reintjens R, Wells A, Massonneau V, Manley J. Key green engineering research areas for sustainable manufacturing: a perspective from pharmaceutical and fine chemicals manufacturers. *Org Process Res Dev.* 2011;15:900–911.
17. Poechlauer P, Manley J, Broxterman R, Gregertsen B, Ridemark M. Continuous processing in the manufacture of active pharmaceutical ingredients and finished dosage forms: an industry perspective. *Org Process Res Dev.* 2012;16:1586–1590.
18. Lightfoot EN. Can membrane cascades replace chromatography? Adapting binary ideal cascade theory of systems of two solutes in a single solvent. *Sep Sci Technol.* 2005;40:739–756.
19. Gunderson SS, Brower WS, O'Dell JL, Lightfoot EN. Design of membrane cascades. *Sep Sci Technol.* 2007;42:2121–2142.
20. Lightfoot EN, Root TW, O'Dell JL. Emergence of ideal membrane cascades for downstream processing. *Biotechnol Prog.* 2008;24:599–605.
21. Abatemarco T, Stickel J, Belfort J, Frank BP, Ajayan PM, Belfort G. Fractionation of multiwalled carbon nanotubes by cascade membrane microfiltration. *J Phys Chem B.* 1999;103:3534–3538.
22. Abejón R, Garea A, Irabien A. Optimum design of reverse osmosis systems for hydrogen peroxide ultrapurification. *AIChE J.* 2012;58: 3718–3730.
23. Overdevest PEM, Hoenders MHJ, van't Riet K, van der Padt A. Enantiomer separation in a cascaded micellar-enhanced ultrafiltration system. *AIChE J.* 2002;48:1917–1926.
24. Ghosh R. Novel cascade ultrafiltration configuration for continuous, high-resolution protein-protein fractionation: a simulation study. *J Membr Sci.* 2003;226:85–99.
25. Cheang B, Zydney AL. A two-stage ultrafiltration process for fractionation of whey protein isolate. *J Membr Sci.* 2004;231:159–167.
26. Isa MHM, Coraglia DE, Frazier RA, Jauregi P. Recovery and purification of surfactin from fermentation broth by a two-step ultrafiltration process. *J Membr Sci.* 2007;296:51–57.
27. Mohanty K, Ghosh R. Novel tangential-flow countercurrent cascade ultrafiltration configuration for continuous purification of humanized monoclonal antibody. *J Membr Sci.* 2008;307:117–125.
28. Mayani M, Mohanty K, Filipe C, Ghosh R. Continuous fractionation of plasma proteins HSA and HIgG using cascade ultrafiltration systems. *Sep Purif Technol.* 2009;70:231–241.
29. Mayani M, Filipe C, Ghosh R. Cascade ultrafiltration systems-integrated processes for purification and concentration of lysozyme. *J Membr Sci.* 2010;347:150–158.
30. Wang L, Khan T, Mohanty K, Ghosh R. Cascade ultrafiltration bioreactor-separator system for continuous production of F(ab′)2 fragment from immunoglobulin G. *J Membr Sci.* 2010;351:96–103.
31. Vanneste J, de Ron S, Vandecruys S, Soare SA, Darvishmanesh S, van der Bruggen B. Techno-economic evaluation of membrane cascades relative to simulated moving bed chromatography for the purification of mono- and oligosaccharides. *Sep Purif Technol.* 2011;80:600–609.
32. Arunkumar A, Etzel MR. Fractionation of alfa-lactalbumin from beta-lactoglobulin using positively charged tangential flow ultrafiltration membranes. *Sep Purif Technol.* 2013;105:121–128.
33. Caus A, Braeken L, Bousus K, van der Bruggen B. Integrated nanofiltration cascades with low salt rejection for complete removal of pesticides in drinking water production. *J Chem Technol Biotechnol.* 2009;84:391–398.
34. Lin JC, Livingston AG. Nanofiltration membrane cascade for continuous solvent exchange. *Chem Eng Sci.* 2007;62:2728–2736.
35. Katraro R, Linder C, Nemas M. *Multi-Stage Membrane System and Process*. US Patent 5676832, 1997.
36. Vanneste J, Ormerod D, Theys G, van Gool D, van Camp B, Darvishmanesh S, van der Bruggen B. Towards high resolution membrane-based pharmaceutical separations. *J Chem Technol Biotechnol.* 2013;88:98–108.
37. Troup GM, Georgakis C. Process systems engineering tools in the pharmaceutical industry. *Comput Chem Eng.* 2013;51:157–171.
38. Morao AIC, Zondervan E, Krooshof G, Geertman R, de Haan AB. Synthesis tool for separation processes in the pharmaceutical industry. *Comput Aided Chem Eng.* 2011;29:276–280.
39. Cervera-Padrell AE, Skovby T, Kiil S, Gani R, Gernaey KV. Active pharmaceutical ingredient (API) production involving continuous processes—a process systems engineering (PSE)-assisted design framework. *Eur J Pharm Biopharm.* 2012;82:437–456.
40. Gernaey KV, Cervera-Padrell AE, Woodley JM. A perspective on PSE in pharmaceutical process development and innovation. *Comput Chem Eng.* 2012;42:15–29.
41. Winkelnkemper T, Schembecker G. Purification fingerprints for experimentally based systematic downstream process development. *Sep Purif Technol.* 2010;71:356–366.
42. Winkelnkemper T, Schembecker G. Purification performance index and separation cost indicator for experimentally based systematic downstream process development. *Sep Purif Technol.* 2010;72:34–39.
43. van Reis R, Saksena S. Optimization diagram for membrane separations. *J Membr Sci.* 1997;129:19–29.
44. Venkiteshwaran A, Belfort G. Process optimization diagrams for membrane microfiltration. *J Membr Sci.* 2010;357:105–108.
45. Haghighatnia Y, Balalaie S, Bijanzadeh, HR. Designing and synthesis of novel amidated fentanyl analogs. *Helv Chim Acta.* 2012;95:818–824.
46. Janssens F, Torremans J, Janseen AJ. Synthetic 1,4-disubstituted-l,4-dihydro-5H-tetrazol-5-one derivatives of fentanyl: alfentanil (R 39209), a potent, extremely short-acting narcotic analgesic. *J Med Chem.* 1986;29:2290–2297.
47. Mathew J, Killgore K. *Methods for the Synthesis of Alfentanil, Sufentanil and Remifentanil*. US Patent 7208604 B2, 2007.
48. Malek A, Hawlader AMN, Ho JC. Design and economics of RO seawater desalination. *Desalination.* 1996;105:245–261.
49. Al-Enezi G, Fawzi N. Design consideration of RO units: case studies. *Desalination.* 2003;153:281–286.
50. Redondo J, Busch M, de Witte JP. Boron removal from seawater using FILMTECTM high rejection SWRO membranes. *Desalination.* 2003;156:229–238.
51. Taniguchi M, Fusaoka Y, Nishikawa T, Kurihara M. Boron removal in RO seawater desalination. *Desalination.* 2004;167:419–426.
52. Abejón R, Garea A, Irabien A. Analysis, modelling and simulation of hydrogen peroxide ultrapurification by multistage reverse osmosis. *Chem Eng Res Des.* 2012;90:442–452.
53. Hidalgo AM, León G, Gómez M, Murcia MD, Barbosa DS, Blanco P. Application of the solution-diffusion model for the removal of atrazine using a nanofiltration membrane. *Desalination Water Treat.* 2013;51:2244–2252.
54. Fierro D, Boschetti-de-Fierro A, Abetz V. The solution-diffusion with imperfections model as a method to understand organic solvent nanofiltration of multicomponent systems. *J Membr Sci.* 2012;413–414:91–101.
55. Kovács Z, Discacciati M, Samhaber W. Modeling of amino acid nanofiltration by irreversible thermodynamics. *J Membr Sci.* 2009; 332:38–49.
56. Pontié M, Dach H, Leparc J, Hafsi M, Lhassani A. Novel approach combining physico-chemical characterizations and mass transfer modelling of nanofiltration and low pressure reverse osmosis membranes for brackish water desalination intensification. *Desalination.* 2008;221:174–191.
57. Abejón R, Garea A, Irabien A. Ultrapurification of hydrogen peroxide solution from ionic metals impurities to semiconductor grade by reverse osmosis. *Sep Purif Technol.* 2010;76:44–51.
58. Machado DR, Hasson D, Semiat R. Effect of solvent properties on permeate flow through nanofiltration membranes Part II. *Transport model. J Membr Sci.* 2000;166:63–69.
59. Darvishmanesh S, Buekenhoudt A, Degrève J, van der Bruggen B. General model for prediction of solvent permeation through organic and inorganic solvent resistant nanofiltration membranes. *J Membr Sci.* 2009;334:43–49.
60. Marchetti P, Butté A, Livingston AG. An improved phenomenological model for prediction of solvent permeation through ceramic NF and UF membranes. *J Membr Sci.* 2012;415–416:444–458.
61. Kedem O, Katchalsky A. Permeability of composite membranes: 1–3. *Trans Faraday Soc.* 1963;59:1918–1953.
62. Fariñas M. *Osmosis Inversa: Fundamentos, Tecnología y Aplicaciones.* Madrid: McGraw-Hill, 1999.
63. Medina San Juan JA. *Desalación de aguas salobres y de mar. Osmosis Inversa.* Madrid: Mundi-Prensa, 2000.

64. Brooke A, Kendrick D, Raman R. *GAMS: A User's Guide (Release 2.50)*. Washington, DC: GAMS Development Corporation, 1998.
65. Bérubé JF, Gendreau M, Potvin JY. An exact epsilon-constraint method for bi-objective combinatorial optimization problems: application to the traveling salesman problem with profits. *Eur J Oper Res*. 2009;194:39–50.
66. Abejón R, Garea A, Irabien A. Multiobjective optimization of membrane processes for chemicals ultrapurification. *Comput Aided Chem Eng*. 2012;30:542–546.
67. Cristóbal J, Guillén-Gosálbez G, Jiménez L, Irabien A. Multi-objective optimization of coal-fired electricity production with CO2 capture. *Appl Energy*. 2012;98:266–272.
68. Abejón R, Garea A, Irabien A. Integrated countercurrent reverse osmosis cascades for hydrogen peroxide ultrapurification. *Comput Chem Eng*. 2012;41:67–76.

Manuscript received Aug. 2, 2013, and revision received Nov. 6, 2013.